Talanta 117 (2013) 75–80

Contents lists available at ScienceDirect

Talanta

journal homepage: www.elsevier.com/locate/talanta

UV–visible-DAD and ^{1}H-NMR spectroscopy data fusion for studying the photodegradation process of azo-dyes using MCR-ALS

Cristina Fernández, M. Pilar Callao *, M. Soledad Larrechi

Department of Analytical and Organic Chemistry, Rovira i Virgili University, C/Marcel·lí Domingo, s/n, Campus Sescelades, E-43007 Tarragona, Spain

ARTICLE INFO

Article history:
Received 29 May 2013
Received in revised form
30 July 2013
Accepted 5 August 2013
Available online 31 August 2013

Keywords:
Azo-dyes
Photodegradation process
UV–visible spectroscopy
Proton-nuclear magnetic resonance spectroscopy
Data fusion

ABSTRACT

The photodegradation process of three azo-dyes – Acid Orange 61, Acid Red 97 and Acid Brown 425 – was monitored simultaneously by ultraviolet–visible spectroscopy with diode array detector (UV–vis-DAD) and ^{1}H-nuclear magnetic resonance (^{1}H-NMR). Multivariate curve resolution-alternating least squares (MCR-ALS) was applied to obtain the concentration and spectral profile of the chemical compounds involved in the process. The analysis of the H-NMR data suggests there are more intermediate compounds than those obtained with the UV–vis-DAD data. The fusion of UV–vis-DAD and the ^{1}H-NMR signal before the multivariate analysis provides better results than when only one of the two detector signals was used. It was concluded that three degradation products were present in the medium when the three azo-dyes had practically degraded. This study is the first application of UV–vis-DAD and ^{1}H-NMR spectroscopy data fusion in this field and illustrates its potential as a quick method for evaluating the evolution of the azo-dye photodegradation process.

1. Introduction

The removal of pollutants from wastewater is a major environmental problem that is being addressed by a variety of disciplines. Azo-dyes are a group of pollutants that require particular attention because they are used in numerous areas and are highly toxic to living organisms [1].

Although many methods have been used to remove organic contaminants from the wastewater of the textile and dye industries, advanced oxidation processes such as photodegradation are the most effective [2]. The initial step in the photodegradation of an azo-compound usually involves a reductive cleavage of the azo-bond, which leads to the formation of toxic aromatic amines. [3,4]. So, to control the wastewater toxicity, both the effectiveness with which the azo-compounds are degraded and the absence of toxic photodegradation intermediates need to be assessed.

Spectroscopic techniques such as UV–visible spectroscopy are usually used to monitor the effectiveness of degradation while chromatographic-mass spectrometry techniques are commonly used for identifying subproducts [2]. In recent years [5–11] methodologies based on the chemometric analysis of the data obtained from spectroscopically monitoring degradation process have proved to be very useful for extracting information about kinetic aspects and the type of intermediate formed. In particular, our research group used multivariate curve resolution-alternating least squares (MCR-ALS) analysis of the UV–vis-DAD data that was recorded during the photodegradation of Acid Orange 61, Acid Red 97 and Acid Brown 425 to perform a kinetic study in order to establish the optimal conditions in which this process should be carried out [5,6].

In the present study the photodegradation process was monitored simultaneously with two spectroscopic techniques – ultraviolet–visible diode array (UV–vis-DAD) and ^{1}H-nuclear magnetic resonance (^{1}H-NMR) – and interpreted by multiset analysis by multivariate curve resolution-alternating least squares (MCR-ALS). When MCR-ALS is applied to data matrices formed by the spectra obtained during the degradation process, it is recovered a profile in each order (concentration and spectra) for each component that is sensible to detector.

The developed strategy constitutes a relatively fast methodology, useful both to monitor the degradation of the three dyes mentioned as for information on the presence of intermediate compounds.

^{1}H-NMR spectroscopy was selected to complement the data which was obtained from UV–vis-DAD because it has some significant advantages over the techniques that are habitually used [12]. It is a nondestructive technique, it does not require the sample to be treated, it gives qualitative and quantitative information, it is fast and it is very suitable for identifying unstable compounds.

Aliquots collected at different reaction times were analyzed simultaneously by the two spectroscopic techniques and the

* Corresponding author. Tel.: +34 977 558 299; fax: +34 97755.
E-mail address: mariapilar.callao@urv.cat (M. Pilar Callao).

0039-9140/$ - see front matter © 2013 Elsevier B.V. All rights reserved.
http://dx.doi.org/10.1016/j.talanta.2013.08.004

spectra were fused so that they could be analyzed by MCR-ALS, and the concentration profile and the pure spectra of the initial azodyes and the products could be obtained. The fusion of the data from both techniques was expected to improve the information provided by a single spectroscopic technique, but for a better illustration of the advantages of this strategy the results of the MCR-ALS analysis using the individual UV–vis-DAD and ^{1}H-NMR data are also included and compared.

Few studies [13] have exploited the potential of data fusion techniques applied to multiway processes and to our knowledge photodegradation process using ^{1}H-NMR and UV–vis-DAD-^{1}H-NMR data fusion and MCR-ALS have not been studied at all. So, this paper is a novelty that may provide important information in the field of photodegradation processes.

2. Experimental

2.1. Chemicals

Acid Orange 61, Acid Red 97 and Acid Brown 425 dyes were obtained from Trumpler Española, S.A. (Barberà del Vallès, Barcelona, Spain). H_2O_2 (30%) was purchased from Scharlau. Degradation solutions were prepared in ultrapure Milli-Q water from a system supplied by Millipore (USA).

2.2. Instruments, measuring conditions and software

2.2.1. Photodegradation reactor

The cylindrical annular batch reactor consisted of a Pyrex glass outer reactor with a capacity of 0.7 L and a quartz immersion tube (2.5 cm i.d. and 38 cm long). The tube contained a 15 W low-pressure mercury-vapour lamp (LPML) (Heraeus Noblelight, Germany). This light source emitted at 254 nm and the incident photon flux of the UV reactor was 0.1 W cm^{-1}.

2.2.2. UV–visible spectrophotometer

Spectral data were acquired using a diode-array spectrophotometer (Shimadzu MultiSpec-1501) and Hyper-UV 1.51 software. The UV–visible spectra of the dye-degradation samples were recorded at each nm from 244 to 720 nm.

2.2.3. ^{1}H-NMR spectrometer

Before the ^{1}H-NMR analysis, samples were vacuum dried in a Lyotrap lyophilizer from LTE Scientific LTD, and the lyophilized samples were dissolved in 600 μL of D_2O (from Euroisotop, France) and placed in 5 mm NMR tubes. ^{1}H-NMR spectra were recorded at 300 K on an Avance III 600 spectrometer (Bruker, Germany) operating at a proton frequency of 600.20 MHz. The spectral width was 12 kHz (20 ppm), and a total of 256 transients were collected at 64k data points for each ^{1}H-NMR spectrum. An exponential line broadening of 0.3 Hz was applied before Fourier transformation. The frequency domain spectra were phased, baseline corrected, and then referenced to a TDP (2,2′,3,3′-tetradeuteropropionic acid) signal, δ=0 ppm, using TopSpin software (version 2.1, Bruker®).

2.2.4. Software

The UV–vis-DAD and ^{1}H-NMR spectra were exported and converted into MATLAB binary files. All data matrices were analysed by MCR-ALS, available in Ref. [14], in a MATLAB 6.5 computer environment [15].

2.3. Photodegradation procedure

A solution of 30 mg L^{-1} of each dye (Acid Orange 61, Acid Red 97 and Acid Brown 425) in Milli-Q water was introduced into the cylindrical reactor and H_2O_2 was added to obtain a final concentration of 0.05 M. The final sample volume was 0.5 L. A total of 23 samples of 5 mL of the degradation solution were taken at the beginning of the experiment (t=0 min) and every 2 min throughout the degradation time (t=44 min). The UV–vis-DAD and ^{1}H-NMR spectra were recorded.

2.4. Chemometric analysis and procedure

MCR-ALS theory has been described in multiple papers, among them include some published by Tauler [16,17]. The aim of this methodology is to decompose the experimental matrices $\mathbf{D_i}$ into two new matrices according to Eq. (1):

$$\mathbf{D} = \mathbf{CS}^{\mathrm{T}} + \mathbf{E} \quad (1)$$

where $\mathbf{C}$ and $\mathbf{S^T}$ contain, respectively, information about the concentration and spectral profiles of species involved in the photodegradation process, which are sensitive to the detector. $\mathbf{E}$ is the matrix of the residuals that contains the variance unexplained by $\mathbf{CS^T}$. MCR-ALS solves the equation iteratively in order to minimize the residual matrix $\mathbf{E}$.

Scheme 1a presents the structure and the MCR-ALS treatment for the individual data matrices, $\mathbf{D_{UV-vis-DAD}}$ and $\mathbf{D_{1H\text{-}NMR}}$, obtained, respectively, from UV–vis-DAD and ^{1}H-NMR spectra recorded during the degradation. The last three rows correspond to the UV–vis-DAD and ^{1}H-NMR pure spectra of the three dyes recorded in the same experimental conditions, and were added to the data matrices, in order to improve the quality of resolution. For the ^{1}H-NMR data, a variable reduction was first carried out by suppressing the values with no signal to obtain $\mathbf{D_{1H\text{-}NMR\text{-}c}}$.

To prevent the ^{1}H-NMR data having much more influence than the UV–vis-DAD data in the analysis, because of their larger absolute values and larger size of the digitized data (5720), before the fusion of the individual data $\mathbf{D_{UV-vis-DAD}}$ and $\mathbf{D_{1H\text{-}NMR\text{-}c}}$, the ^{1}H-NMR data were scaled and the number of variables for each spectrum were reduced (Scheme 1b). The value of each is the sum of the values of 10 consecutive original variables. In this step we obtain the $\mathbf{D_{1H\text{-}NMR\text{-}SR}}$ matrix. The augmented data matrix $\mathbf{D_{aug}}$ indicated in Scheme 1c was formed, by combining the $\mathbf{D_{UV-vis-DAD}}$ and $\mathbf{D_{1H\text{-}NMR\text{-}sr}}$ matrices in the row wise direction.

The application of MCR-ALS requires the compound number involved in the photodegration process (c_1, c_2 or c_3 in the Scheme) and their spectral or concentration profiles to be estimated.

The number of chemical compound involved in each experiment, c_1 and c_2, was assessed by means of the singular value decomposition (SVD) [18] of each individual data matrix, $\mathbf{D_{UV-vis-DAD}}$ and $\mathbf{D_{1H\text{-}NMR\text{-}c}}$, according to Eq. (2):

$$\mathbf{D} = \mathbf{USV}^{\mathrm{T}} \quad (2)$$

The diagonal values of $\mathbf{S}$ are known as the singular values of $\mathbf{D}$, and the columns of both, $\mathbf{U}$ and $\mathbf{V^T}$, are the left-singular vectors and right-singular vectors of $\mathbf{D}$, respectively.

We used simple-to-use interactive self-modeling mixture (SIMPLISMA) [19,20] of the individual data matrices $\mathbf{D_{UV-vis-DAD}}$ and $\mathbf{D_{1HNMR\text{-}c}}$ to obtain the initial estimation of the spectral profile. These initial estimates were iteratively optimized by a constrained alternating least squares (ALS) regression procedure.

The aim of the optimization process was to minimize the value of the residual matrix ($\mathbf{L}$). The constraints applied were non-negativity for both the concentration and spectral profile, unimodality for the concentration profiles and normalization of the spectral profiles.

The quality of the MCR-ALS resolution was evaluated using the lack of fit (LOF), the percentage of explained variance (R^2) and the

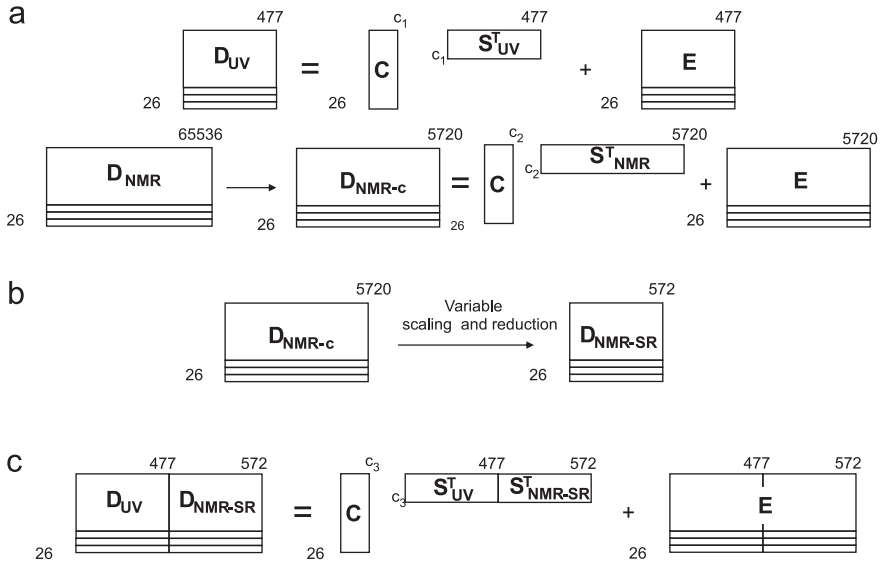

Scheme 1. Structure and MCR-ALS treatment for the experimental data matrices.

similarity (or correlation) coefficient (r):

$$\mathrm{LOF}(\%) = 100 \times \sqrt{\frac{\sum e_{ij}^2}{\sum d_{ij}^2}} \tag{3}$$

$$R^2(\%) = \left(1 - \frac{\sum d_{ij}^2 - \sum e_{ij}^2}{\sum d_{ij}^2}\right) \times 100 \tag{4}$$

$$r = \cos\gamma = \frac{s_i^T \hat{s}_i}{\|s_i\| \times \|\hat{s}_i\|} \tag{5}$$

where d_{ij} is an element of the experimental data matrix **D**; e_{ij} is the related residual obtained from the difference between the experimental data and the reproduced data by the resolution model; γ is the angle defined for the vectors associated with the recovered profile by MCR-ALS ($\hat{s}_i$) and the real profile (s_i).

Two different LOF values are calculated, according to the defined input data matrix **D** (taken either as the raw experimental data matrix or the PCA reproduced data matrix, using the same number of components as the MCR-ALS model). The better fit of the experimental data is when the values of LOF, R^2 and r are closer to zero, hundred and one, respectively.

To determine the c_3 value, the system was solved iteratively using values between c_1 and c_2. We selected the number of factors that provided a solution with the best quality parameters.

3. Results and discussion

Fig. 1 shows UV–vis-DAD and ^{1}H-NMR spectra of the samples obtained at the beginning, at two intermediate times and at the end of the photodegradation process. Fig. 1a shows a decrease in the absorbance values, which is much more pronounced in the visible zone. From this figure it follows that when dyes are removed, the species that absorb in the UV range remain in solution, but from the shape of the spectrum the number and type of substances that cause this signal cannot be deduced.

Fig. 1b shows the ^{1}H-NMR spectra. In the spectrum at time zero, the chemical shifts between 1 and 4.5 ppm, which are characteristic of aliphatic protons, can be observed.

The disappearance of the signal at a chemical shift of 5.4 ppm (attributable to the phenol group present in the three dyes) and the weak, broad signals at chemical shifts around 7.5 ppm (characteristic of aromatic protons) may indicate that, in the presence of H_2O_2, oxidation of the phenolic groups occurs from the beginning to form quinones [21].

An increase of the signal around 8.3 ppm (attributable to the hydroperoxide group) is observed. This is in agreement with a progressive degradation of the dyes through diazonium intermediates to produce phenols and their oxidation species (the hydroperoxides) as described in the literature [22]. At the end of the process, only these signals were detected.

The important signal observed between 4.5 and 5 ppm is attributable to the H_2O contained in the solutions analyzed. So, this zone was removed to prevent erroneous results.

It is difficult to determine how many compounds are involved in the degradation process by visual inspection of both types of spectra alone. Below, the information from the MCR-ALS analysis of the individual data matrices and of the fused matrices is discussed.

3.1. Individual study

First, in each ^{1}H-NMR spectrum of the $\mathbf{D}_{1\text{H-NMR}}$ data matrix, the δ signals close to zero and the δ values around 5 ppm were removed from the analysis. So, we obtained a new data matrix $\mathbf{D}_{1\text{H-NMR-c}}$ with a dimension of 26×5720.

The choice of the number of factors is performed considering that the number should be equal to or greater than three (initial species) and by the inspection of eigenvalues and the percentage of variance calculated by SVD analysis of the individual data matrices (both $\mathbf{D}_{\text{UV–vis-DAD}}$ and $\mathbf{D}_{1\text{H-NMR-c}}$). Table 1 shows these values for the first 10 factors. It can see that, for the $\mathbf{D}_{\text{UV–vis-DAD}}$ data matrix, from the fourth factor the variations of the eigenvalue are non significant. When the magnitude of the eigenvalue for the $\mathbf{D}_{1\text{H-NMR}}$, data matrix is inspecting, it is not easy detect an inflexion point to consider the value representative of the noise. So, we decided retained successively different number of factor, always higher than four, and resolve the system to analyze the solution considering other quality parameters.

The most satisfactory results were obtained with 7 factors. MCR-ALS was applied considering 4 factors for UV–vis-DAD data and 7 for ^{1}H-NMR data.

The difference in number of factors between the two sets of data can be interpreted considering that the intermediates formed in the process of degradation should be groups naphthalenes and

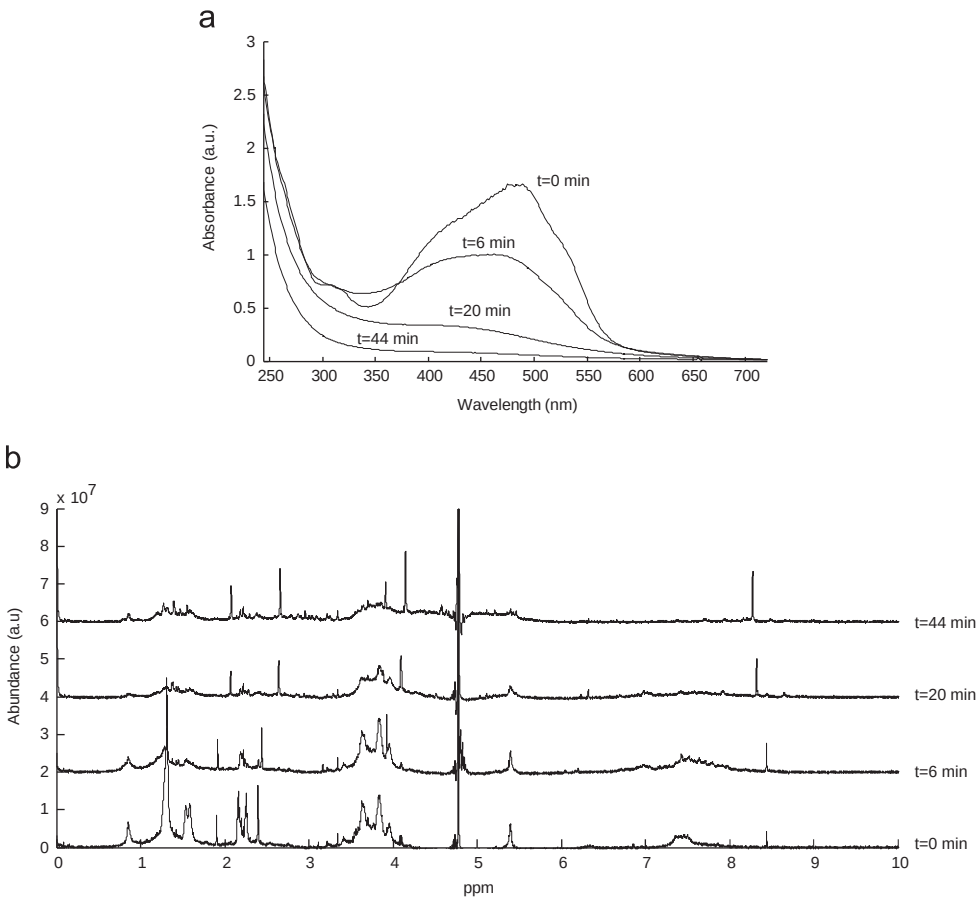

Fig. 1. Spectra recorded during the photodegradation process (a) by UV–vis-DAD spectroscopy, (b) by ^{1}H-NMR spectroscopy.

Table 1
Eigenvalue and cumulative variance from SVD analysis.

Component	Eigenvalues ^{1}H-NMR ($\times 10^9$)	% Cumulative variance	Eigenvalues UV–vis	% Cumulative variance
1	1.3109	71.43	56.8073	92.61
2	0.4543	80.01	15.6054	99.60
3	0.3631	85.49	3.6354	99.98
4	0.2838	88.84	0.7731	100.00
5	0.2436	91.31	0.1740	100.00
6	0.1967	92.92	0.1298	100.00
7	0.1708	94.13	0.1128	100.00
8	0.1466	95.02	0.0855	100.00
9	0.1355	95.79	0.0626	100.00
10	0.1340	96.53	0.0564	100.00

benzenesulphonics not distinguishable each other in the UV region. Fig. 2 shows the concentration profiles obtained after MCR-ALS resolution. The first two columns in Table 2 show the quality parameters of the resolution in both cases.

Fig. 2a shows that the most persistent dye was the brown one, which was still present until approximately 30 min. It can also be observed that an intermediate was formed from the very beginning of the degradation, and that the concentration of this compound increased for 20 min, after which time it also degraded and no signal corresponding to the new degradation products could be observed. All the quality parameters of this resolution, expressed in the second column of Table 2, are satisfactory. However, we should point out that the spectrum of the orange dye has a lower correlation coefficient than the other dyes. This may indicate that the corresponding concentration profile does not fit perfectly.

The quality parameters of the resolution with the ^{1}H-NMR data show that the model contains a significant lack of fit (errors and variance explained) and provides low spectral correlation values. The information obtained from Fig. 2b should be interpreted with this in mind. It is surprising that that the concentration of Acid Red 97 seems to increase during the first minutes and then decreases. Also, the first intermediate does not appear until the 12th minute of degradation. One explanation for this is that the resolution confuses the different compounds, especially the spectrum of Acid Red 97 and the spectrum of an initial intermediate. In the later stages of the process, new species (or new situations that keep changing) appear. A comparison of the results of the two techniques shows that when the data are more complex it is more difficult to obtain a good model fit. The use of ^{1}H-NMR enables qualitative information to be obtained about the intermediates (up to four can be observed) but the concentration profiles are not in agreement with the previous results and the quality parameters obtained are not satisfactory either.

3.2. Data fusion (UV–vis-DAD and ^{1}H-NMR)

Because of the large difference in the scale of the signals, before fusion the ^{1}H-NMR spectra data were normalized to values between 0 and 1. The UV–visible spectra data did not have to be normalized because they were already in this order of magnitude. In addition, in ^{1}H-NMR data, a variable reduction was carried out by eliminating the variables with no signal. We performed an initial MCR-ALS treatment with results that were similar to those obtained when only ^{1}H-NMR was used, because about 10 times more variables were used from ^{1}H-NMR than from UV–vis-DAD.

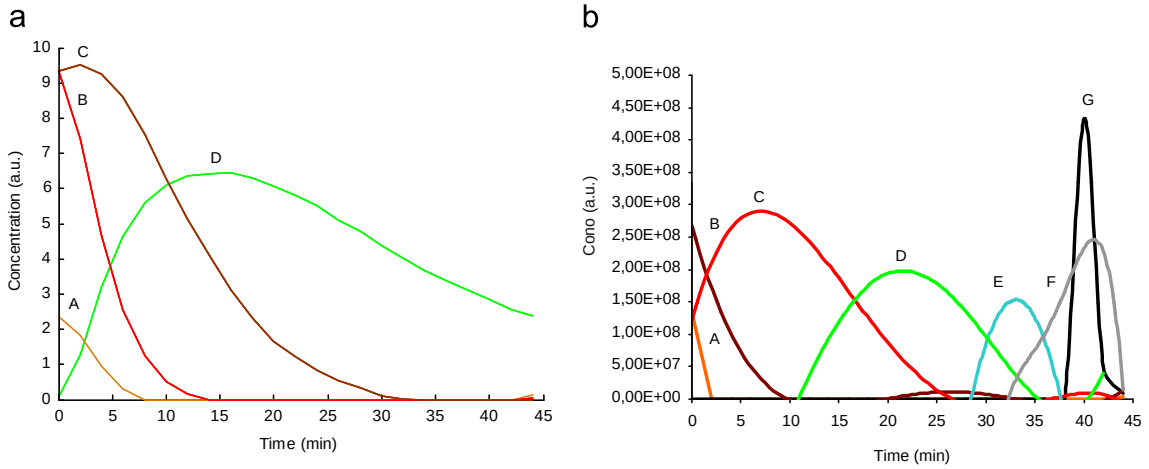

Fig. 2. Concentration profiles retrieved by MCR-ALS resolution for (a) UV–vis-DAD degradation matrix, (b) ^{1}H-NMR degradation matrix. (For interpretation of the references to color in this figure legend, the reader is referred to the web version of this article.)

Table 2
Parameters of quality of all the MCR-ALS resolutions.

	UV–vis–DAD	^{1}H NRM	Fusion	
Factor number	4	7	6	
LOF (PCA)	9.1144	2.73256	**5.9532**	
LOF (Exp)	9.2574	3.62578	9.5102	
R^2	9.9143	8.68537	9.90956	
r Red 97	0.9999	0.8904	0.9985[a]	0.9588[b]
r Acid Orange 61	0.9040	0.7447	**0.9786**[a]	0.7917[b]
r Acid Brown 425	0.9921	0.8242	**0.9957**[a]	0.7616[b]

[a] UV–vis–DAD spectra.
[b] ^{1}H NMR spectra.

We tried a variety of strategies to reduce the number of ^{1}H-NMR variables [23,24] and results were best when we used new variables that were the sum of the 10 consecutive original variables. Finally, we obtained the modified ^{1}H-NMR spectra data matrix ($\mathbf{D_{NMR\text{-}SR}}$) in Scheme 1b, with 572 variables, a similar number of the UV–visible spectra.

The data fusion, according to Scheme 1c, was resolved with 4–7 factors. The best and most chemically interpretable results were obtained with 6 factors. The quality parameters of the resolution and the correlation coefficient between the pure spectra of the dyes and those retrieved by MCR-ALS are shown in the third and fourth column of Table 2. Fig. 3 shows the concentration and spectral profiles. In this figure, letters A–C correspond respectively to Acid Orange 61dye, Acid Red 97 dye and Acid Brown 425 dye. Letters D–F correspond to different reaction intermediates.

From the data in Table 2 it can be deduced that the quality parameters in the fusion resolution are in the same order of quality as those obtained when only individual techniques are used or better. The results that are better than those of UV–visible spectroscopy and ^{1}H-NMR are marked in bold and underlined, respectively. It should be noted that the quality of ^{1}H-NMR-resolved spectra is still insufficient. This may be due to the complexity present in the NMR data.

The concentration profiles, expressed in arbitrary unit, (Fig. 3a) show that for approximately the first 15 min the information obtained is similar to that obtained with UV–vis-DAD: they show the disappearance of the three colorants and the appearance of the first degradation product. After 15 min this product decreases and a second product forms and remains until the end of the process. In the final minutes, a new degradation product appears and disappears. It can be observed that the sum of the first two intermediates has the shape of the concentration profile of the only intermediate observed in UV–vis-DAD resolution (Fig. 2a).

Fig. 3b shows the spectral profiles retrieved for the UV–vis-DAD matrix. The spectra of Acid Orange 61 (λ_{max}=446 nm), Acid Red 97 (λ_{max}=498 nm) and Acid Brown 425 (λ_{max}=445 nm) could be identified. However, the spectrum previously identified as an intermediate product (not shown) is now split into two spectra, the intermediate D presents absorbance in the visible region (λ_{max}=425 nm), and the intermediate E mainly absorbs in the UV region (λ_{max}=280 nm). This is attributed to small intermediates obtained in the photodegradation of the first intermediate. The last component F does not absorb in the UV–vis region.

Fig. 3c shows the spectral profiles for ^{1}H-NMR. It has to be taken into account that the representation corresponds to the sum of 10 consecutive points, which makes it difficult to interpret the intermediates present. Nevertheless an approximate pathway can be established. We can observe the ^{1}H-NMR spectra of the three dyes A–C, in which the more important peak appears in the region of the aliphatic protons (δ=1–4.5 ppm). The D intermediate has high peaks at 8.4 ppm, at 4 ppm and at 1.1 ppm. As mentioned above the signal at 8.4 ppm can be attributed to the hydroperoxide group. The signal at 4 ppm is typical of aromatic amines that can be formed from the cleavage of azo linkages. The signal at 1.1 ppm can be attributed to aliphatic CH_2. The high peaks present in the D intermediate are not observed in the E intermediate, probably because the D intermediate degrades to other molecules and aromaticity is lost. The F intermediate spectrum, which appears only at the end of the degradation (Fig. 3a) when the recovered concentration for the initial azo-dyes is nule, shows high peaks in zones coinciding with those of the above species. Considering that the main products at the end of the photodegradation processes are H_2O and CO_2, whose signals are removed in the data pretreatment, the F spectrum peaks can be attributed to impurities that remain in the solution. Also, at this point, it is necessary to remember that the MCR-ALS are dotted of ambiguity [25], which affect both, the concentration and the spectra profile.

From the results shows in Fig. 3 we can postulate that the pathway involves the oxidation of dye molecules, the cleavage of azo-linkages and, finally, the degradation of intermediates. This is in agreement with other studies carried out with different dyes and MS spectrometry [4,26].

4. Conclusions

The results show the complexity of the azo-dye photodegradation process. The MCR-ALS analysis of the UV–vis-DAD data is a very

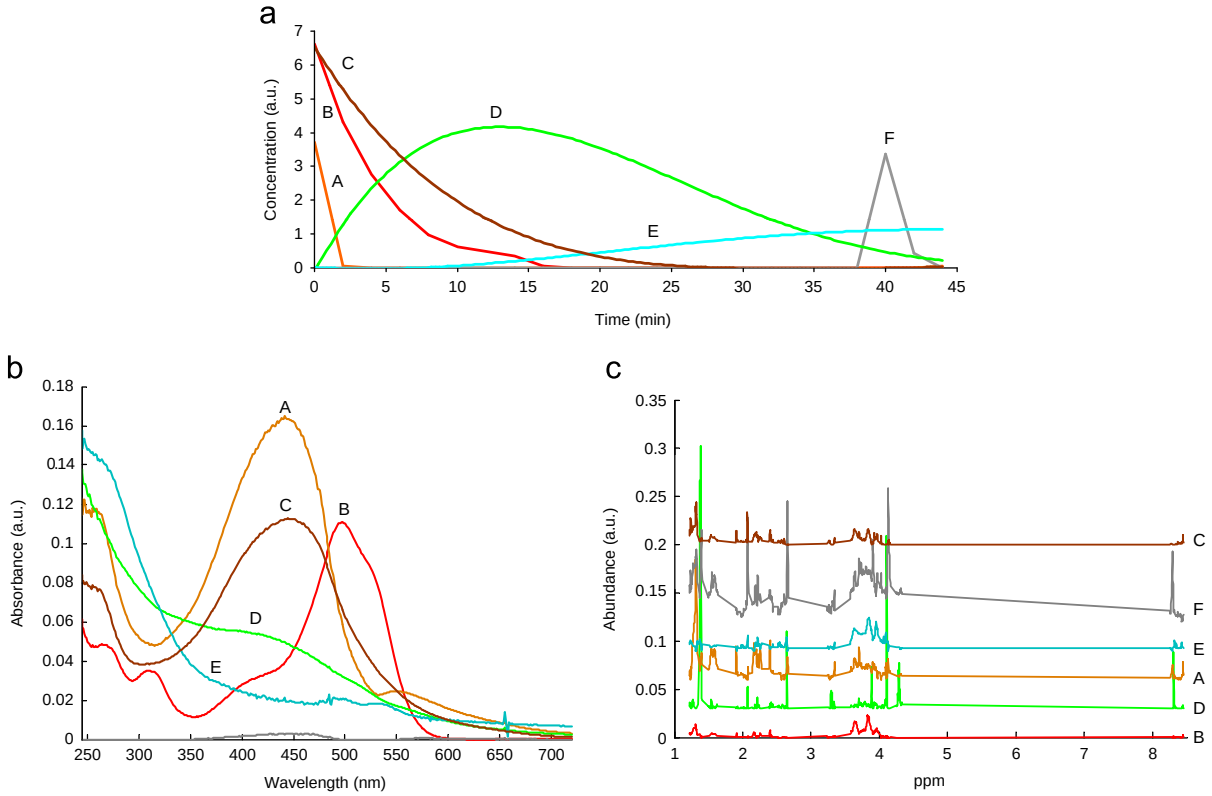

Fig. 3. Profiles retrieved by MCR-ALS resolution of the fused data. (a) UV–vis-DAD spectra (b) ^{1}H-NMR spectra, (c) concentration profiles. (For interpretation of the references to color in this figure legend, the reader is referred to the web version of this article.)

useful tool to monitor the simultaneous degradation of each azo-dye but the information provided about the intermediates is very limited.

The MCR-ALS analysis of the ^{1}H-NMR data suggests the presence of four intermediate products throughout the process. However, watching the process under study, the concentration profiles obtained are meaningless for the initial dyes, so it can be inferred that ^{1}H-NMR spectroscopy is a technique that provides information that complements that which is obtained by UV–vis-DAD spectroscopy

The application of MCR-ALS to fused UV–vis-DAD and ^{1}H-NMR data resolves the system with six factors, indicative of at least six compounds throughout the process. The concentration profiles obtained suggest that three compounds are present in the medium when the concentration of the pure azo-dye is practically null, who is according to the expected in terms of the degradation process.

The spectra obtained are in agreement with a process that involves the asymmetrical cleavage of the azo-linkages of the dyes to give hydroxyperoxides. Additional techniques will be required if the intermediates involved in this process are to be accurately elucidated. However, from a practical point of view this information is not always required, usually only is necessary detected if the degradation products do not remain in the medium. In this regard, the methodology used in the present study can be considered as a good alternative.

The fusion of the UV–vis data with 1HNMR have allowed joint to MCR-ALS represent a clear advantage respect to use any of both techniques independently.

Acknowledgements

The authors would like to thank the Agency for the Administration of University and Research of the Catalan Government (AGAUR) for economic support (project 2009 SGR 549).

References

[1] R.O. Cristóvao, A.P.M. Tavares, L.A. Ferreira, J.M. Loureiro, R.A.R. Boaventura, E.A. Macedo, Bioresour. Technol 100 (2009) 1094–1099.
[2] C. Fernández, M.S. Larrechi, M.P. Callao, Trends Anal. Chem. 29 (2010) 1202–1211.
[3] L. Wojnàrovits, E. Takàcs, Radiat. Phys. Chem. 77 (3) (2008) 225–244.
[4] C. Fernández, M.P. Callao, M.S. Larrechi, J. Hazard. Mater. 190 (2011) 986–992.
[5] C. Fernández, M.S. Larrechi, M.P. Callao, Talanta 79 (2009) 1292–1297.
[6] C. Fernández, M.S. Larrechi, M.P. Callao, J. Hazard. Mater. 180 (2010) 474–480.
[7] C. Fernández, A. de Juan, M.P. Callao, M.S. Larrechi, Chemom. Intell. Lab. Syst. 114 (2012) 64–71.
[8] M.V. Bosco, M.S. Larrechi, Talanta 71 (2007) 1703–1709.
[9] M Bosco, M.P. Callao, M.S. Larrechi, Talanta 72 (2007) 800–807.
[10] A. Jayaraman, S. Mas, R. Tauler, A. de Juan, J. Chromatogr. B 910 (2012) 138–148.
[11] V. Gómez, J. Font, M.P. Callao, Talanta 71 (2007) 1393–1398.
[12] I.K. Konstantinou, T.A. Albanis, Appl. Catal., B 49 (2004) 1–14.
[13] S. Mas, R. Tauler, A. de Juan, J. Chromatogr. A 1218 (2011) 9260–9268.
[14] ⟨http://www.ub.es/gesq/mcr/mcr.htm⟩.
[15] Matlab 6.5, The Mathworks, South Natick, MA, USA.
[16] R. Tauler, Chemom. Intell. Lab. Syst. 30 (1995) 133–146.
[17] A. de Juan, M. Maeder, M. Martínez, R. Tauler, Chemom. Intell. Lab. Syst. 54 (2000) 123–141.
[18] D.L. Massart, B. Vandeginste, L. Buydens, S. de Jong, P. Lewi, J. Smeyers-Verbeke, Handbook of Chemometrics and Qualimetrics: Part A, first ed., Elsevier, Amsterdam, 1997.
[19] W. Windig, J. Guilment, Anal. Chem. 63 (1991) 1425–1432.
[20] W. Windig, Chemom. Intell. Lab. Syst. 36 (1997) 3–16.
[21] J. March, Advanced Organic Chemistry: Reactions, Mechanism and Structure, fifth ed., Wiley, New York, 2001.
[22] C. López, A. Valade, B. Combourieu, I. Mielgo, B. Bouchon, J.M. Lema, Anal. Biochem 335 (2004) 135–149.
[23] L. Nørgaard, A. Saudland, J. Wagner, J.P. Nielsen, L. Munck, S.B. Engelsen, Appl. Spectrosc. 54 (2000) 413–419.
[24] C di Anibal, I. Ruisánchez, Talanta 86 (2011) 316–323.
[25] R. Tauler, A. Smilde, B.R. Kowalski, J. Chemom. 9 (1995) 31–58.
[26] B. Kayan, Belgin Gözmen, M. Demirel, A.M. Gizir, J. Hazard. Mater 177 (2010) 95–102.